# The effect of temperature on creep and physical ageing of poly(vinyl chloride)

**P. E. Tomlins*, B. E. Read and G. D. Dean**
*Division of Materials Metrology, National Physical Laboratory, Teddington, Middlesex TW11 0LW, UK*
*(Received 7 October 1993)*

Tensile creep data have been obtained for poly(vinyl chloride) at a number of temperatures ranging from 21.5 to 58°C. The results were obtained from specimens of different age characterized by the elapsed time $t_e$ between quenching a sample from 85°C to the test temperature and the start of the creep test. A model for interpreting non-linear creep data has been developed to describe the creep behaviour of the material as a function of both age and temperature. The results show that the effect of physical ageing is to progressively reduce the level of the relaxed $\beta$ compliance and to increase the mean retardation time of the glass–rubber $\alpha$ relaxation process. The effect of conducting creep tests on specimens of the same age at progressively higher temperatures is the opposite: the level of the relaxed $\beta$ compliance increases whilst the mean retardation times of the $\alpha$ process decrease. Neither the ageing rate nor the shape of the distribution of retardation times are affected by temperature.

**(Keywords: physical ageing; poly(vinyl chloride); creep)**

## INTRODUCTION

The onset of the glass–rubber $\alpha$ retardation process in poly(vinyl chloride (PVC) at 23°C occurs within the time range of 0.1–10 s and is predicted to reach completion after approximately $10^{14}$ s ($3 \times 10^6$ years), as revealed by tensile creep measurements[1]. This $\alpha$ process is superposed on a $\beta$ retardation process associated with a secondary relaxation, which is active over a timescale of $10^{-10}$–10 s, as shown schematically in *Figure 1*.

In a previous study of PVC[2] we investigated the effects of physical ageing on the creep behaviour of these two retardation processes at constant temperature and described them in terms of empirical functions with age-dependent parameters. The age of a glassy material ($t_e$) is defined as the storage time at the test temperature between quenching from some elevated temperature $T_0$ (where $T_0 > T_g$) and the instant of load application. The influence of physical ageing on the $\beta$ process is to reduce the magnitude of the relaxed compliance $D_{R\beta}$, whilst the mean retardation time $\tau_\beta$ and the parameter characteristic of the width of the retardation-time spectrum remain unchanged. In contrast, it appears that for the $\alpha$ process the mean retardation time $t_0$ depends on the age of the material, shifting to longer times as the material becomes older. However, both the magnitude of the $\alpha$ compliance and the width of the retardation-time spectrum characterized by a parameter $\gamma$ remain constant.

Tensile creep tests conducted on testpieces of different ages fall into two categories, short-term and long-term. In a short-term test the age of the sample on completion of the test remains effectively unchanged, as the creep time $t$ is short, typically $(0.2–0.3)t_e$. This is not the case for a long-term test, where the test period is typically $(10–30)t_e$. Thus in a short-term test the mean retardation time $t_0$ is effectively constant, whereas in a long-term test it progressively increases with creep time beyond the short-term region of $(0.2–0.3)t_e$.

The tensile creep compliance data $D(t)$ obtained from creep tests conducted over a limited range of time from a variety of amorphous polymers of different age states can be accurately described by the function:

$$D(t) = D_{R\beta} \exp(t/t_0)^\gamma \qquad (1)$$

assuming $t_e$ and hence $t_0$ to be constant. This function has been extensively used by Struik and others[1,3] and is consistent with the stress relaxation function $\exp[-(t/t_0)^\gamma]$ proposed by Kohlrausch[4,5]. In a long-term test for creep times in excess of $0.3t_e$, where $t_0$ progressively increases with time, the Struik–Kohlrausch function becomes:

$$D(t) = D_{R\beta} \exp\left(\int_0^t \frac{du}{t_0(u)}\right)^\gamma \qquad (2)$$

where the parameters $D_{R\beta}$ and $\gamma$ are the same as those used in equation (1) and $u$ is a dummy time variable. A function to describe $t_0(t)$ is developed and discussed at length below.

In this paper we present tensile creep data at a number of temperatures for PVC with a view to modelling long-term data and to determining the temperature dependence of the parameters required by equation (2) and its associated functions.

* To whom correspondence should be addressed

0032-3861/94/20/4376–06

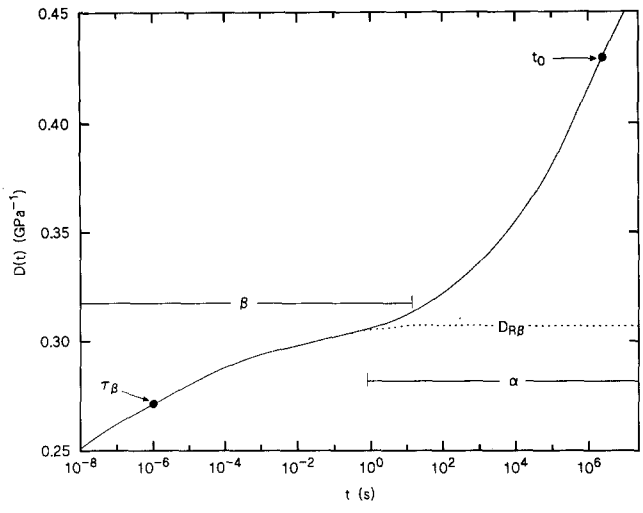


**Figure 1** A schematic diagram illustrating the superposition of the $\alpha$ glass–rubber relaxation process on the $\beta$ secondary relaxation mechanism for PVC at room temperature. $\tau_\beta$ and $t_0$ are the mean retardation times for each process and $D_{R\beta}$ is the relaxed $\beta$ compliance, which is equivalent to the unrelaxed $\alpha$ compliance

## EXPERIMENTAL

The PVC (ICI, Darvic) was obtained from Amari Plastics, UK, in the form of a 6 mm thick transparent sheet. The measured density of the material prior to any heat treatment was found to be 1387 kg m$^{-3}$ at 23°C. Typical dimensions of testpieces machined from the sheet (using water as a coolant) were $12 \times 6 \times 180$ mm. Prior to testing, the specimens were heated to 85°C for a period of 30 min in order to erase previous ageing effects. They were then quenched into water at the test temperature for a period of approximately 5 min, dried and stored in air at the same temperature for various periods of elapsed time $t_e$ before creep measurements were made.

Tensile creep data for times $>1$ s were obtained for all temperatures spanning the range 21.5–58°C using rigs located within temperature-controlled chambers situated within a temperature-controlled room. The long-term stability of the temperature within each chamber was typically $\pm 0.2$°C. Constant loads applied to each testpiece produced a stress of 5 MPa, which is very close to the onset of non-linearity in the stress–strain curve.

## RESULTS AND DISCUSSION

### *Analysis of short-term data*

*Figure 2* shows the effects of both temperature and elapsed time on the short-term tensile creep behaviour of PVC. For any given creep time $t$, the compliance $D(t)$ decreases with increasing age of the testpiece. Similarly for samples of the same age the compliance at a given creep time increases with increasing test temperature.

Equation (1) can be used to describe such short-term creep behaviour providing the parameters $D_{R\beta}$, $t_0$ and $\gamma$ are known. In a previous study of PVC[2] at 23°C, values of $D_{R\beta}$ were obtained by modelling data spanning the $\beta$ relaxation with a symmetrical Cole–Cole function. This approach requires creep data over a wide timescale, in our case $10^{-8}$–1 s, which were obtained by using a variety of dynamic mechanical techniques. However, recent work has shown[6,7] that accurate values of $D_{R\beta}$ may be obtained without the need for very short-time data, at least for PVC, where there is little overlap between the $\alpha$ and $\beta$ relaxations.

This is achieved by writing equation (1) as:

$$\ln D(t) = \ln D_{R\beta} + (t/t_0)^{\gamma} \tag{3}$$

which is then differentiated with respect to $\ln t$ so that:

$$\frac{d \ln D(t)}{d \ln t} = \gamma \ln D(t) - \gamma \ln D_{R\beta} \tag{4}$$

The derivative $d \ln D(t)/d \ln t$ is obtained by differentiating a power series polynomial equation used to fit a plot of $\ln D(t)$ against $\ln t$, as shown in the inset of *Figure 3*. A plot of the derivative *versus* $\ln D(t)$ is also shown in *Figure 3*, where the slope is $\gamma$ and the intercept on the abscissa is $\ln D_{R\beta}$. The $\gamma$ values obtained by linear least-square fits to the data of the derivative plots for all elapsed times and temperatures were found within experimental error to be independent of both variables. A constant value of $0.32 \pm 0.02$ was therefore chosen for $\gamma$. The $D_{R\beta}$ values appropriate to this constant were generated by fitting

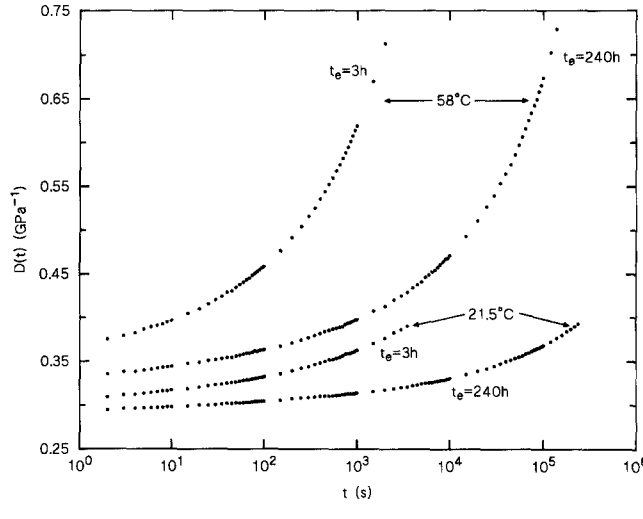


**Figure 2** The influence of both temperature and elapsed time on the creep behaviour of PVC

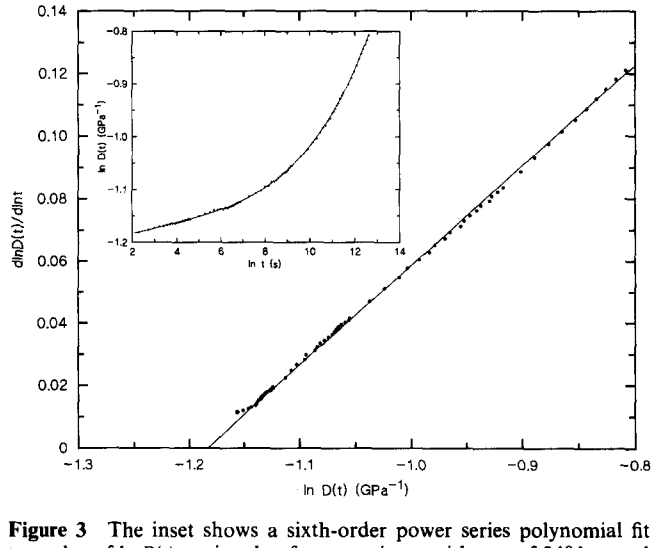


**Figure 3** The inset shows a sixth-order power series polynomial fit to a plot of $\ln D(t)$ against $\ln t$ for a specimen with a $t_e$ of 240 h tested at 33.2°C. The main figure shows a linear least-squares fit to a plot of the derivative of the polynomial with respect to $\ln t$ *versus* $\ln D(t)$. The slope of the line is $\gamma$ (0.32) and the intercept yields $D_{R\beta}$ (0.306)

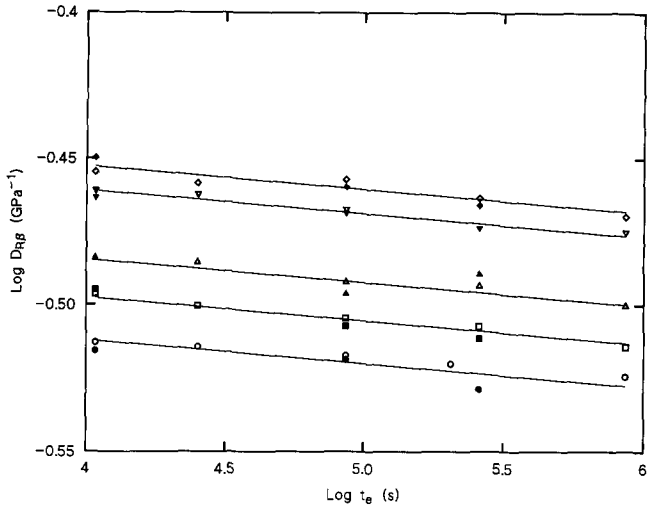


**Figure 4** Plots of $\log D_{R\beta}$ *versus* $\log t_e$ for different temperatures. The open symbols refer to data obtained from short-term tests whilst the filled symbols refer to data obtained from the short-term parts of long-term tests. The slopes of the linear least-squares fits to the data give a constant value for $v$ ($8.1 \times 10^{-3}$) and the intercepts yield temperature-dependent values for $W$ (see *Table 1*). Symbols: (○, ●) 21.5°C, (□, ■) 33.2°C, (△, ▲) 44.5°C, (▽, ▼) 51.0°C and (◇, ◆) 58.0°C

**Table 1** Temperature-dependent values of $W$, $A$ and $C$ for $v = 8.1 \times 10^{-3}$ and $\mu = 0.86$ respectively

| Temp. (±0.2°C) | $W$ ($GPa^{-1} s^{v}$) | $A$ ($s^{1-\mu}$) | $C$ ($s^{1-\mu}$) |
|---|---|---|---|
| 21.5 | 0.331 | 98.4 | 95.2 |
| 33.2 | 0.343 | 42.2 | 34.8 |
| 44.5 | 0.353 | 16.0 | 12.25 |
| 51.0 | 0.373 | 7.0 | 6.61 |
| 58.0 | 0.380 | 2.5 | 2.45 |

slopes of 0.32 to plots of $\mathrm{d}\ln D(t)/\mathrm{d}\ln t$ *versus* $\ln D(t)$ for each of the elapsed times at each temperature.

*Figure 4* shows the variation of $D_{R\beta}$ with both elapsed time and temperature. The data are consistent with a function of the form:

$$D_{R\beta} = W(T) t_e^{-v} \quad (5)$$

It is apparent from this figure that, whilst the slope $v$ can be considered as independent of temperature, the intercept $W$ (*Table 1*) cannot, and its temperature dependence is described below.

Values of $t_0$ may be obtained by rewriting equation (1) as:

$$\{\ln[D(t)/D_{R\beta}]\}^{1/\gamma} = t/t_0 \quad (6)$$

and plotting the left-hand side of the equation against creep time $t$. Such a plot is shown in the inset of *Figure 5* for the short-term region of a long-term test, where it is apparent that a linear relationship exists between the two variables over a period of creep time $t_s$. Over this timescale both $t_0$ and $t_e$ are effectively constant and equation (1) applies. *Figure 6* is a plot of the $t_0$ values obtained using equation (6) for both short-term tests and the short-term regions of long-term tests conducted on specimens of different $t_e$ at different temperatures.

A relationship of the form:

$$t_0 = A(T) t_e^{\mu} \quad (7)$$

may be used to describe the data, where the ageing rate $\mu$, given by the slope of a plot of $\log t_0$ *versus* $\log t_e$, can be regarded as being independent of temperature ($\mu = 0.86 \pm 0.10$), although it should be noted that there is some indication that $\mu$ exhibits a slight maximum at 50°C. These findings are in good agreement with those of Struik[1], who determined the tensile creep behaviour of rigid PVC over a comparable temperature range for elapsed times ranging from 0.2 to 16 h. However, there is evidence to suggest that this value for $\mu$ is only applicable over a limited range of short elapsed times[1,2] possibly reflecting some curvature in a plot of $\log t_0$ against $\log t_e$ over a wide range of $t_e$. The temperature dependence of $A$ (given in *Table 1*) is discussed below.

*Analysis of long-term data*

From *Figure 5* it is apparent that the linear relationship between $t_0$ and $\{\ln[D(t)/D_{R\beta}]\}^{1/\gamma}$ breaks down beyond a

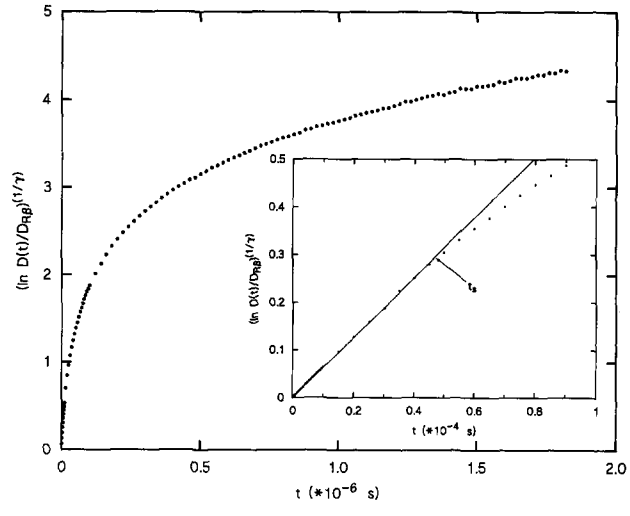


**Figure 5** The inset shows the period of creep time over which the relationship between $\{\ln[D(t)/D_{R\beta}]\}^{1/\gamma}$ and $t$ is linear (equation (6)) for a sample with a $t_e$ of 3 h tested at 51°C. The slope of this plot is $t_0^{-1}$ (where $t_0 = 1.6 \times 10^4$ s). Beyond the creep time $t_s$ this linear relationship breaks down, as shown in both the main figure and inset, as $t_e$ and hence $t_0$ progressively increase with time

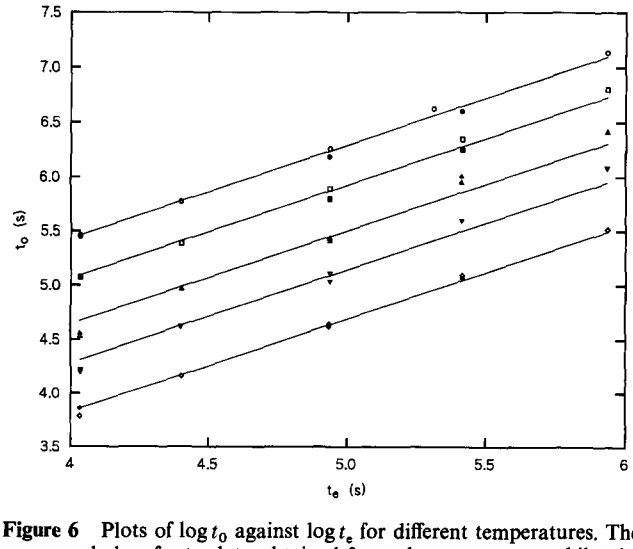


**Figure 6** Plots of $\log t_0$ against $\log t_e$ for different temperatures. The open symbols refer to data obtained from short-term tests whilst the filled symbols refer to data obtained from the short-term parts of long-term tests. The slopes of the linear least-squares fits to the data give a constant value for $\mu$ (0.86) and the intercepts yield temperature-dependent values of $A$. Symbols: (○, ●) 21.5°C, (□, ■) 33.2°C, (△, ▲) 44.5°C, (▽, ▼) 51.0°C and (◇, ◆) 58.0°C

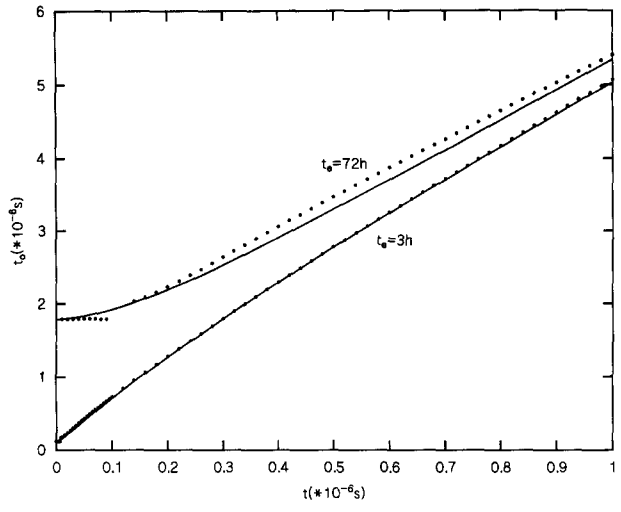


**Figure 7** A comparison of the predicted time dependence of $t_0$ generated by equation (9) (—) and that derived from experimental data (●) using equation (8) for the elapsed times of 3 and 72 h at 33.2°C. Note the convergence of the $t_0$ values from both sets of data at long times towards a curved asymptote

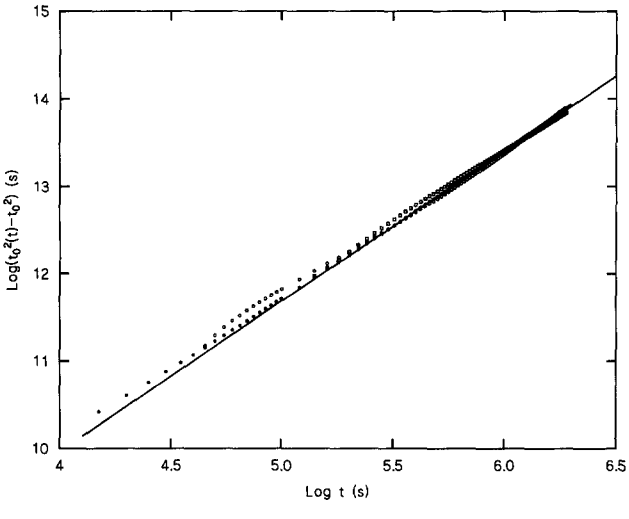


**Figure 8** Plots of $\log[t_0^2(t)-t_0^2]$ *versus* $\log t$ for three elapsed times at 33.2°C: (●) 3 h, (○) 24 h, (□) 72 h. The full line fit to the data based on equation (9) has a slope $\mu=0.86$ and an extrapolated intercept $C$ of 34.8 $s^{1-\mu}$

creep time $t_s$, which reflects the limit of the short-term region of the creep curve. However, values for $t_0$ as a function of time can still be obtained from the slope of this plot by differentiation. In order to avoid undue bias to the data at very long times, it is convenient to differentiate $\{\ln[D(t)/D_{R\beta}]\}^{1/\gamma}$ with respect to log time and hence:

$$\frac{d\{\ln[D(t)/D_{R\beta}]\}^{1/\gamma}}{d\log t}=\frac{2.303t}{t_0} \quad (8)$$

An estimate of the derivative can easily be obtained by differentiating a power series polynomial used to describe a plot of $\{\ln[D(t)/D_{R\beta}]\}^{1/\gamma}$ against $\log t$ for times greater than $t_s$. *Figure 7* shows a plot of $t_0$ *versus* time for two elapsed times at 33.2°C. The initial horizontal portions represent the period of time over which both $t_e$ and $t_0$ are effectively constant. Subsequently $t_0$ progressively increases with time as a result of further ageing, with the values converging at longer times as the initial differences in the ages of the testpieces become less significant. Such curves resemble a family of hyperbolae approaching a common curved asymptote, which is concave to the time axis. This behaviour can be described by a general function of the form:

$$t_0^2(t)=t_0^2+C^2(T)t^{2\mu'} \quad (9)$$

where $t_0$ now represents the initial value of $t_0(t)$.

From equation (9) a plot of $\log[t_0^2(t)-t_0^2]$ against $\log t$ should therefore be linear with a slope of $2\mu'$ and an intercept of $2\log C(T)$. *Figure 8* shows such a plot for a long-term test conducted at 33.2°C using testpieces with initial $t_e$ values of 3, 24 and 72 h. The slope $\mu'$ was found to be equivalent, within experimental error, to the value of $\mu$ determined from the short-term data and similarly was found to be independent of both temperature and elapsed time. The parameter $C$ can be considered as being independent of elapsed time but strongly dependent on temperature (*Table 1*) as will be discussed below.

By substituting the hyperbolic function (equation (9)) into equation (2) we obtain:

$$D(t)=D_{R\beta}\exp\left(\int_0^t \frac{du}{(t_0^2+C^2u^{2\mu'})^{0.5}}\right)^{\gamma} \quad (10)$$

where the integral needs to be solved by a numerical method[8].

*The temperature dependence of the parameters* W, A *and* C

*Figure 9* illustrates the temperature dependence of $W$, the parameter that describes the temperature dependence of the relaxed $\beta$ compliance (equation (5)). These data may be represented by a function of the form:

$$W(T)=a_0+a_1T+a_2T^2 \quad (11)$$

which contains the empirical constants $a_0$ (0.32 $GPa^{-1}s^{\gamma}$), $a_1$ ($-1.62\times10^{-4}$ $GPa^{-1}s^{\gamma}°C^{-1}$) and $a_2$ ($1.94\times10^{-5}$ $GPa^{-1}s^{\gamma}°C^{-2}$).

The dependences of $\log A$ and $\log C$ on inverse temperature (in K) are shown in *Figure 10*. Although the plots are significantly curved at higher temperatures due to the onset of the glass–rubber transition, over the range 20–50°C the data can be described by linear Arrhenius plots.

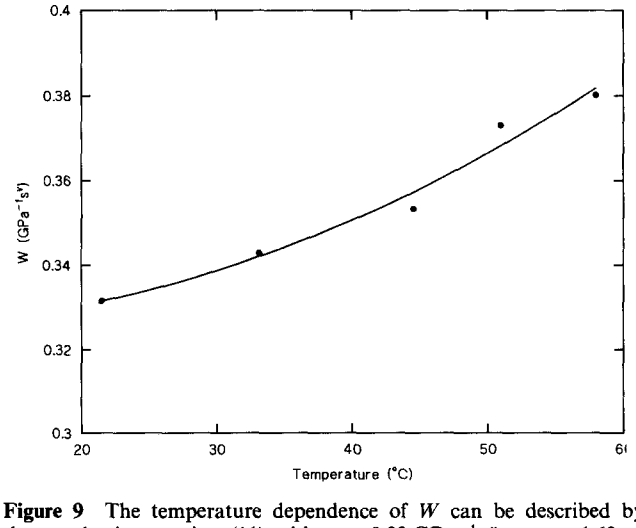


**Figure 9** The temperature dependence of $W$ can be described by the quadratic equation (11) with $a_0=0.32$ $GPa^{-1}s^{\gamma}$, $a_1=-1.62\times10^{-4}$ $GPa^{-1}s^{\gamma}°C^{-1}$ and $a_2=1.94\times10^{-5}$ $GPa^{-1}s^{\gamma}°C^{-2}$

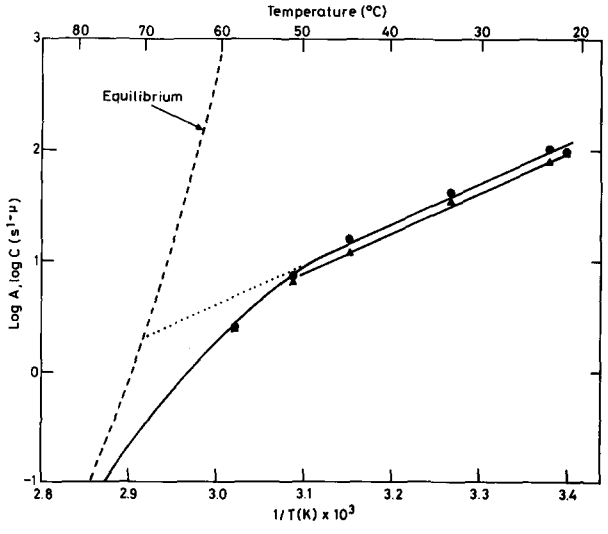


**Figure 10** The inverse temperature dependence of $\log A$ (●) and $\log C$ (▲)

These data may be interpreted on the basis of the Adam–Gibbs function as applied to the non-equilibrium glassy state[9], noting that in this case the relaxation times at each temperature pertain to elapsed times of 1 s. Then

$$A(T)=A'\exp\left[\frac{B}{T}\left(\frac{T_f}{T_f-T_2}\right)\right] \quad (12)$$

and

$$C(T)=A'\exp\left[\frac{B}{T}\left(\frac{T_{fc}}{T_{fc}-T_2}\right)\right] \quad (13)$$

where $A'$ and $B$ are constants, $T_f$ and $T_{fc}$ are fictive temperatures and $T_2$ is the temperature at which the configurational entropy is predicted to vanish.

D.s.c. measurements have shown that the glass transition occurs over the range of 50–80°C for rapidly quenched PVC (Darvic) with a glass transition temperature of approximately 70°C. This latter value can be used as an approximation to a test-temperature-invariant fictive temperature $T_f$ in equation (12) and (13). Then assuming that $T_f-T_2$ has the 'universal' value of 51.6 K (hence $T_2=291.4$ K), $B$ (=1265 K) and $A'$ ($=4.52\times10^{-11}$ s$^{1-\mu}$) can be determined from the respective slope and intercept (at $1/T=0$) of the linear part of the $\log A$ *versus* $1/T$ plot.

The broken curve of *Figure 10* is the predicted equilibrium line obtained using the derived values of $A'$ and $B$ together with either equation (12) or (13), which at equilibrium both reduce to the Vogel–Fulcher form:

$$A(T)=A'\exp\left(\frac{B}{T-T_2}\right) \quad (14)$$

The intersections of the equilibrium line with the extrapolated linear portions of the $\log A$ and $\log C$ *versus* $1/T$ plots occur at the fictive temperatures $T_f$ and $T_{fc}$ respectively (where $T_{fc}$ is 70.4°C). The slight disparity between $T_f$ and $T_{fc}$ may be attributable to the assumption that $\mu$ is independent of temperature, which results in different values of $A$ being obtained from those determined when $\mu$ is a variable.

*Comparison of measured and predicted long-term creep curves*

By substituting equations (5) and (7) for $D_{R\beta}$ and $t_0$ respectively into equation (10) we obtain:

$$D(t)=W(T)t_e^{-\nu}\exp\left(\int_0^t \frac{du}{[A^2(T)t_e^{2\mu}+C^2(T)u^{2\mu}]^{0.5}}\right)^{\gamma} \quad (15)$$

This function may then be used to calculate long-term creep compliance curves by employing the expressions for $W(T)$, $A(T)$ and $C(T)$ given by equations (11), (12) and (13) respectively.

*Figure 11* shows a comparison of experimental data with results predicted by equation (15) and its associated functions for three elapsed times at 21.5°C. The convergence of these creep curves at long creep times is ascribed to the declining importance of the $t_0^2$ term in equation (9), which at very long times can be ignored. In *Figure 12* the temperature dependence of a family of creep curves is shown for a single elapsed time of 24 h. It should be noted that the fictive temperature used to calculate $A(T)$ and $C(T)$ for the data in this figure at 58°C was taken to be 71.3°C. This value is somewhat higher than that used to calculate $A(T)$ and $C(T)$ over the temperature range 21.5–50°C due to this temperature being in the glass transition region. The divergence of the creep curves

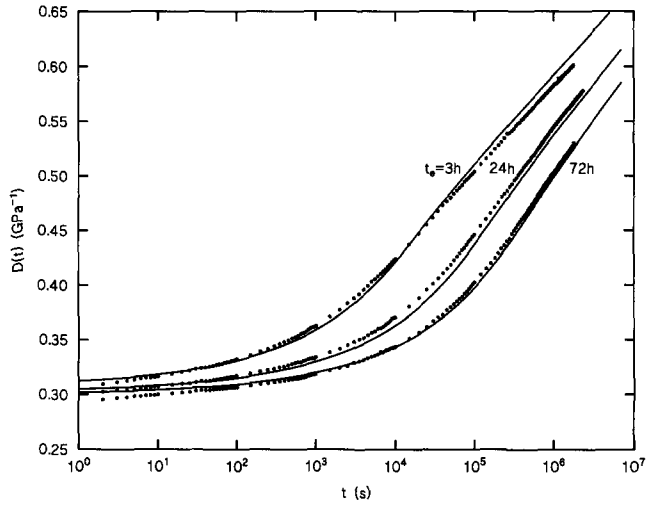


**Figure 11** Long-term creep curves at 21.5°C for the elapsed times indicated. The full curves were calculated from equation (15) using parameters generated by equations (11), (12) and (13)

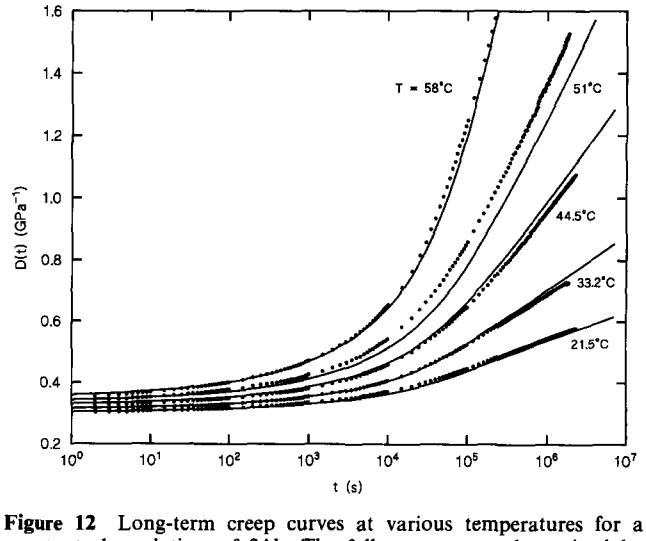


**Figure 12** Long-term creep curves at various temperatures for a constant elapsed time of 24 h. The full curves were determined by equation (15) using parameters obtained from equations (11), (12) and (13)

with creep time reflects that fall of $C(T)$ with increasing temperature, which may arise from a decrease in ageing rate or age state during long-term creep.

The discrepancies between the predicted creep curve and those determined experimentally in *Figures 11* and *12* are quite small and reflect the scatter and reproducibility of data obtained in both long- and short-term tests.

The model presented here could form the basis for predicting creep of polymers over wide and continuous ranges of $t$, $t_e$ and $T$ from data obtained over limited ranges of these variables. However, some aspects of the model, in particular, the assumption that $\mu$ is independent of temperature, need to be validated over a wider range of temperatures than studied here and for other polymers. Previous work has shown that it can vary substantially with temperature for some polymers over wide temperature ranges[1]; however, it may be the case that, over the 'working ranges' of these materials, this can be ignored.

## CONCLUSIONS

The long-term creep behaviour of PVC specimens of different starting ages at different temperatures can be described by equation (10), which principally models the changes in an effective retardation time $t_0$ with creep time. The initial value of $t_0$ depends on the starting age of the material (equation (7)) and the test temperature (equations (7) and (12)). During long-term creep tests $t_0$ progressively increases with time (equation (9)) at a rate that depends on temperature (equation (13)).

## ACKNOWLEDGEMENTS

The research reported in this paper was carried out as part of the 'Materials Measurement Programme', a programme of underpinning research financed by the United Kingdom Department of Trade and Industry.

## REFERENCES

1 Struik, L. C. E. 'Physical Aging in Amorphous Polymers and Other Materials', Elsevier, Amsterdam, 1978
2 Read, B. E., Dean, G. D., Tomlins, P. E. and Lesniarek-Hamid, J. L. *Polymer* 1992, **33**, 2689
3 Lee, A. and McKenna, G. B. *Polymer* 1990, **31**, 423
4 Plazek, D. J., Ngai, K. L. and Rendell, R. W. *Polym. Eng. Sci.* 1984, **24**, 1111
5 Leaderman, H. 'Elastic and Creep Properties of Filamentous Materials and Other High Polymers', Textile Foundation, Washington, DC, 1944, pp. 13–14
6 Dean, G. D., Read, B. E., Lesniarek-Hamid, J. L. and Tomlins, P. E. *Plast. Rubb. Compos. Process. Applic.* 1992, **17**, 225
7 Dean, G. D., Tomlins, P. E. and Read, B. E. NPL Report DMM(A)91, March 1993
8 For this study NAG Fortran Library routine D01 AHF was employed to evaluate numerical integrals (Mark 15, **1**, 1991 NAG Ltd, Oxford)
9 Hodge, I. M. *Macromolecules* 1986, **19**, 936